International Journal of Applied Engineering Research ISSN 0973-4562 Volume 13, Number 18 (2018) pp. 13932-13939

Performance Upper Bounds of High Altitude Platform Systems over a Two-State Switched Channel

Hien Thi Thu Nguyen[1], Hung Viet Nguyen [1], Thang Nhat Le[2]

[1] *Faculty of Telecommunications 1, Posts and Telecommunications Institute of Technology, Km10, Nguyen Trai Street, Ha Dong District, Hanoi, Vietnam.*

[2] *Postgraduate Studies Faculty, Posts and Telecommunications Institute of Technology, Km10, Nguyen Trai Street, Ha Dong District, Hanoi, Vietnam.*

Abstract

This paper presents performance upper bounds of High Altitude Platform (HAP) systems over two-state switched channel model with QPSK modulation. We propose the modified trellis diagram for punctured convolutional code to derive performance upper bounds of HAP systems using IrCC-URC-QPSK coding scheme. This coding scheme achieves better performance than coding scheme in CAPANINA project [1]. Furthermore, the results of upper bounds are also the basis for further verification of the effectiveness of the IrCC-URC-QPSK coding scheme.

Keywords: High Altitude Platform, Upper bounds, Serial Concatenated Convolutional Code, Two-State switched channel model, Bit error probability.

INTRODUCTION

The demand for wireless communication is increasing day by day. People want a high speed of communication in less time. Everyone wants a fast communication from anywhere to anyone. Even rural area also requires internet facility. It is too hard to establish a Base station for particular small village for broadband communication or any wireless communication. Even it's too costly to launch a satellite for particular rural area. So High Altitude Platform (HAP) broadband communication is expected to become a popular solution for the wireless communications infrastructure [2]. HAP networks have been increasingly playing an important role in supporting broadband wireless communication systems, namely fourth generation Long Term Evolution (4G-LTE) and fifth generation (5G) networks [3]. HAPs are communication facilities situated at an altitude of 17 to 30 km and at a particular point relative to the Earth. They have the capability of carrying diverse relay payload supporting multipurpose communications. HAPs in a fully deployed configuration are capable of providing services and applications ranging from broadband wireless access, navigation and positioning systems, remote sensing and weather observation/monitoring systems, mobile telephony as well as digital TV [4].

Nowadays, there are no recommendations on the specific coding and modulation used in the HAP system. Though, there have been several studies evaluating the performance of HAP using a parallel concatenated convolutional codes (PCCC), serial concatenated convolutional codes (SCCC) coding scheme and LDPC [1],[5]. However, these studies only evaluate performance by simulation without theoretical performance analysis. Based on the coding scheme proposed in [1], we propose a coding scheme that uses an irregular convolution code (IrCC) [6] in an outer encoder to increase the channel capacity-near efficiency. To achieve this, we use the EXIT chart tool [7],[8],[9] to select subcodes with different code rates and determine the percentage of information bits encoded by these subcodes. These subcodes are formed by adding more generators (13, 11) and puncturing for lower rates or only puncturing higher rates while maximizing the free distance from memory-3 mother code defined by generators (17, 15). With the simulation results of the proposed coding scheme, we will derive analytical upper bounds to the performance of it. For simplicity, the conventional union bound technique is used in this paper.

Against this background, the novel contribution of this paper is that we make use of the union bound technique [10,11] to derive performance upper bounds of HAP systems over a two-state switched channel model. First, we propose the modified trellis diagram for punctured convolutional code to find the transfer function and weight enumenator. Then, we derive the performance upper bounds for IrCC-URC-QPSK coding scheme with subcodes having various code rates. The derived performance bounds are compared with simulation results to further demonstrate the performance of the designed code.

The paper is structured as follows. Section 2 presents two-state switched channel model for HAP system. Section 3 derive analytical upper bounds to the bit-error probability of HAP systems using a SCCC coding scheme over the two-state switched channel. The conclusion is given in Section 4.

Two-state switched channel model for HAP

Let us now consider a single transmission link between an HAP and a high-speed moving train in CAPANINA project [1] that associated with the transmitted and received signals of x and y, respectively. The received signal can be represented as

$$y = hx + n \tag{1}$$

where $h=h_s.h_f$ is the complex-valued fading coefficient that

fluctuates on a symbol-by-symbol basis, and *n* is the AWGN process having a variance of $N_0/2$ per dimension.

In order to account for different propagation conditions in this scene, a two-state switched model was considered in [1]. It is a Markov model characterized by two states, good (G) and bad (B). Good conditions correspond to a Rice fading model, while bad channel condition corresponds to a Rayleigh distributed fading. As far as the Rice fading model is concerned, the Rician factor K is determined from measurements [12]. Suffice it to say that for rural environments it takes on values on the order of 20dB, while for suburban environments it is K = 10dB. Indeed, the latter value of K has been used in this paper for system performance verification.

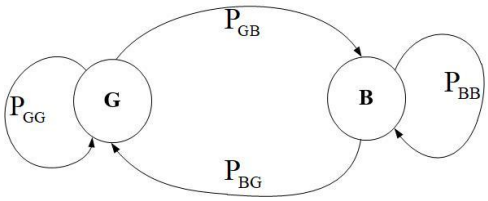

Figure 1: Two-state switched channel model for HAP in CAPANINA project [1].

We assume that states of channel are selected at the beginning of the transmission. The first state (G) with stationary probability π_G=0.565 considers frequency-flat uncorrelated real Rician fading channel with Rice factor K = 10dB, while the second state (B) consider frequency-flat uncorrelated real Rayleigh fading conditions with stationary probability π_B =1-π_G =0.435. But once a channel state is selected, it will not change for the entire transmission period.

Performance upper bounds of HAP systems over a two-state switched channel model

In this section, a channel coding schemes for HAP are proposed and evaluated. Our channel coding scheme (IrCC-URC-MOD) is SCCC coding scheme consists of a irregular convolutional code (IrCC) and a rate-1 convolutional code (URC) that joined by an interleaver of length N bits, the outer code (IrCC) with rate R_c is a irregular convolutional code contained eight subcodes with code rates from 0.2 to 0.9. These subcodes are formed from mother code that is eight-state (17,15) recursive, systematic convolutional encode. URC is a one-state (3,2) recursive, systematic convolutional encoder (Fig.2).

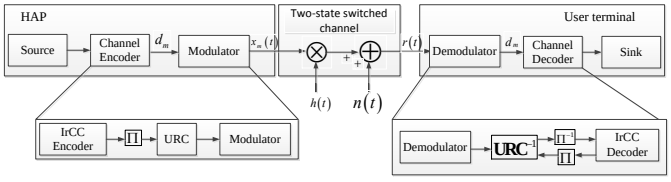

Figure 2: IrCC-URC-MOD Coding Scheme for HAP system.

As seen in Fig. 2, at the transmitter side, an information frame of *N* bits are encoded by the CC encoder, in order to produce an output frame having a frame length of N/R_c bits. The frame is then interleaved before being encoded again by the URC encoder. The frame from output of the URC encoder is modulated by a modulation scheme employing η bits for presenting a symbol, before transmitting to a receive side. At the receiver side, the signals received during a single frame are de-mapped then decoded by the URC decoder before entering the iteratively decoding process of *J* iterations occurring between the URC decoder and the convolutional decoder.

For 8-subcode IrCC, we denote these subcodes with the tuples

$$\{r_i,[w_0,w_1,...],l_i,[p_0,p_1,...]\}$$

where $i=1,2,...8$ or 17 , w_j, $j=0,1,2,3$ denotes the frequency of occurrence of g_j in the generator matrix, l_i is the puncturing period and p_i is the puncturing pattern associated to g_j (in octal) as follow [13]:

$$\{0.2,(1,2,1,1),1,(1,1,1,1)\},\{0.3,(1,1,1,1),3,(7,7,7,1)\},$$
$$\{0.4,(1,1,1),2,(3,3,1)\},\{0.5,(1,1),1,(1,1)\},$$
$$\{0.6,(1,1),3,(7,3)\},\{0.7,(1,1),7,(177,025)\},$$
$$\{0.8,(1,1),4,(17,1)\},\{0.9,(1,1),9,(777,1)\}.$$

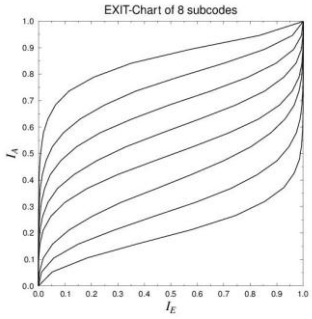

Figure 3: EXIT chart of 8 subcodes from mother code CC(1,15/17).

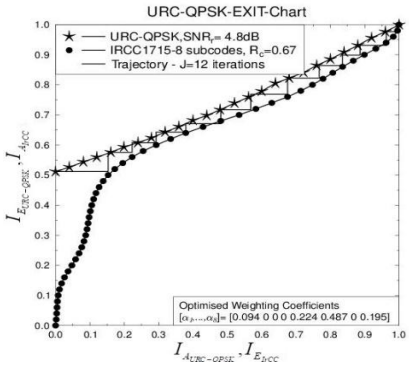

Figure 4: EXIT chart for 8-subcode IrCC(17,15)-URC-QPSK at R_c=0.67.

For code rate R_c=0.67, we use 4 subcodes with code rates 0.2, 0.6, 0.7 and 0.9. Furthermore, we also determine weighting coefficients of 8-subcode IrCC(17,15) $[\alpha_1, \alpha_2, ..., \alpha_8]$=[0.094 0 0 0 0.224 0.487 0 0.195]. It means that each subcode encodes a fraction of $\alpha_i r_i N$ input information frame to $\alpha_i N$ code bits, where α_i, r_i are weight and code rate of i^{th} subcode respectively, N is number of information bits, $i = [1, 2, ..., \Phi]$ with Φ =8.

As SCCC are linear, so union bound can be used to obtain an analytic expression for the probability of error. Assume that input of SCCC is a sequence of N bits consisted of L information bits and K-1 tail bits. A weight enumerator $\mathrm{W}(B, D)$ is defined for the terminated SCCC as

$$\mathrm{W}(B, D) = \sum_i \sum_m c_{i,m} . B^i D^m \tag{1}$$

Without loss of generality, we assume that the all-zero codeword was sent, and we write the upper bound on bit error probability [14] as

$$P_b \le \frac{1}{N} \sum_m \sum_i i . c_{i,m} . P_{m,\text{Two-state switched}}(X, X) \tag{2}$$

where $c_{i,m}$ is the number of error events composed of a single error event with output Hamming distance m and input Hamming distance i and is given by

$$c_{i,m} = \sum_{l=0}^{N} \frac{c_{b,l}^{o} . c_{l,d}^{i}}{\binom{N}{l}} \tag{3}$$

where $c_{b,l}^{o}$ is the number of error events composed of a single error event with output Hamming distance l and input Hamming distance b of outer coder; $c_{l,d}^{i}$ is the number of error events composed of a single error event with output Hamming distance d and input Hamming distance l of inner coder and $P_{m,\text{Two-state switched}}(X, X)$ is the pairwise error probability of the transmitted sequence X and the estimated sequence X over two-state switched channel.

Note that equation (2) stems from the union bound that is based on the fact that the probability of the union of a number of individual events is less than or equal to the sum of probabilities of the individual events. The sums of the individual probabilities of the equations are not probabilities themselves and can assume values greater than one. The bounds are also based on maximum-likelihood decoding, whereas the SCCCs are decoded using a different, suboptimum algorithm. This apparent inconsistency can be resolved through heuristic validation from a large number of simulations, which show the convergence of the simulated performance toward the analytical bounds for large random interleavers [14].

Consider the QPSK signal constellation shown in Fig. 5. Assume that the all zero message is transmitted ($x_i = -\frac{1}{\sqrt{2}} + j\frac{1}{\sqrt{2}}$). Let X differ from X by exactly m symbols, which consist of m_1 symbols of $S_1 = \pm\left(\frac{1}{\sqrt{2}} + j\frac{1}{\sqrt{2}}\right)$ and m_2 symbols of $S_2 = \left(\frac{1}{\sqrt{2}} - j\frac{1}{\sqrt{2}}\right)$.

A weight enumerator $\mathrm{W}(B, D_1, D_2)$ is defined for the terminated SCCC using QPSK modulation scheme as

$$\mathrm{W}(B, \mathrm{D}_1, D_2) = \sum_i \sum_{m_1} \sum_{m_2} c_{i,m_1,m_2} . B^i D_1^{m_1} D_2^{m_2} \tag{4}$$

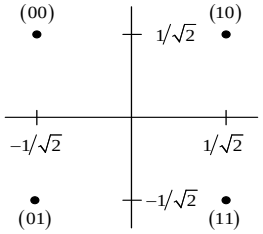

Figure 5: QPSK signal constellation

Then the upper bound on bit error probability is given by

$$P_b \le \frac{1}{N} \sum_{m_1} \sum_{m_2} \sum_i i . c_{i,m_1,m_2} . P_{m_1 m_2, QPSK, \text{Two-state switched}}(X, X) \tag{5}$$

where c_{i,m_1,m_2} is the number of error events composed of a single error event with output Hamming distances m_1, m_2 and input Hamming distance i and is given by

$$c_{i,m_1,m_2} = \sum_{l=0}^{N} \frac{c_{b,l}^{o} . c_{l,d_1,d_2}^{i}}{\binom{N}{l}} \tag{6}$$

where $c_{b,l}^{o}$ is the number of error events composed of a single error event with output Hamming distance l and input Hamming distance b of outer coder; c_{l,d_1,d_2}^{i} is the number of error events composed of a single error event with output Hamming distances d_1, d_2 and input Hamming distance l of inner coder and $P_{m,QPSK,\text{Two-state switched}}(X, X)$ is the pairwise error probability of the transmitted sequence X and the estimated sequence X over two-state switched channel.

Weight enumerator of subcodes formed from mother code CC(1,15/17)

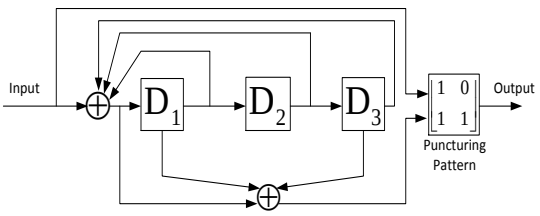

Figure 6: Diagram of encoder CC(1,15/17) with code rate R_c=0.67.

Consider a convolutional encoder (1,15/17) with 3 bit memory elements, code rate R_c=0.67 (Fig.6). In this case, assume that the rate ½ convolutional code CC(17,15) is punctured with a puncturing pattern p_3 = [1 1;0 1] and puncturing period l=3 to obtain rate 0.67 convolutional code CC(1,15/17). It means that the third coded symbols are punctured. To obtain the weight enumerator for computing upper bounds of bit error probability, it is necessary to do as follows:

(i) We produce a modified trellis diagram of convolutional code with a certain code rate (e.g. CC(1,15/17), R_c=0.67 in Fig.7b) from trellis diagram of mother convolutional code (e.g CC(1,15/17), R_c=0.5 in Fig.7a) combined with given puncturing pattern and puncturing period. Specially, we label the branches between two states with the powers of B and L. The exponent of B denotes the Hamming distance between the input sequence, that generated the codeword sequence in question, and the all-zero input sequence. The exponent of D is the Hamming distance between the coded branch output and an all zero branch output. Furthermore, for each trellis depth t = 1 to (N + K - 1) compute

$$\mathrm{F}_{\mathrm{S}_t}(B,L) = \sum_{S_{t-1}=\Lambda_{S_t}} \mathrm{F}_{\mathrm{S}_{t-1}}(B,L).\mathrm{G}_{\mathrm{S}_{t-1},\mathrm{S}_t}(B,L)$$

where $\mathrm{F}_{\mathrm{S}_t}(B,L)$ denotes the coefficients of the polynomial of state S_t at depth t; $G_{\mathrm{S}_{t-1},\mathrm{S}_t}(B,L)$ is the label of the branch between the state S_{t-1} at depth t-1 and the state S_t at depth t; and S_t is the set of states at depth t of the trellis diagram, $\mathrm{S}_t = \left(0,...,2^{K-1}-1\right)$.

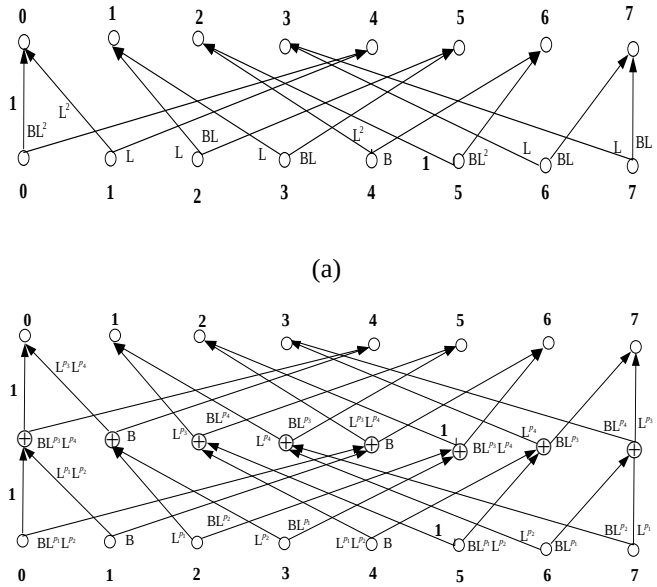

(a)

(b)

Figure 7: Trellis Diagram of CC(1,15/17) with code rate R_c= 0.5 (a) and R_c=0.67 (b).

(ii) We split the zero state into two separate states, namely the start state S_0 and the end state S_0', as depicted in Fig.8.

We then express each state of the diagram as a function of the other states, so as to obtain the state equations:

$$S_0' = \mathrm{L}^2 S_1 + \mathrm{L}^2 S_2 + \mathrm{L}^2 S_3$$

$$S_1 = \mathrm{L}^2 S_4 + S_5 + \mathrm{L}^2 S_6 + \mathrm{L}^2 S_7$$

$$S_2 = \mathrm{BL}^3 S_0 + \mathrm{BL} S_1 + \mathrm{BL} S_2 + \mathrm{BL} S_3$$

$$S_3 = \mathrm{BL} S_4 + \mathrm{BL}^3 S_5 + \mathrm{BL} S_6 + \mathrm{BL} S_7$$

$$S_4 = \mathrm{BL} S_0 + \mathrm{BL}^3 S_1 + \mathrm{BL} S_2 + \mathrm{BL} S_3$$

$$S_5 = \mathrm{BL}^3 S_4 + \mathrm{BL} S_5 + \mathrm{BL} S_6 + \mathrm{BL} S_7$$

$$S_6 = \mathrm{B}^2\mathrm{L}^2 S_0 + \mathrm{B}^2\mathrm{L} S_1 + \mathrm{B}^2\mathrm{L}^2 S_2 + \mathrm{B}^2\mathrm{L}^2 S_3$$

$$S_7 = \mathrm{B}^2 S_4 + \mathrm{B}^2\mathrm{L}^2 S_5 + \mathrm{B}^2\mathrm{L}^2 S_6 + \mathrm{B}^2\mathrm{L}^2 S_7$$

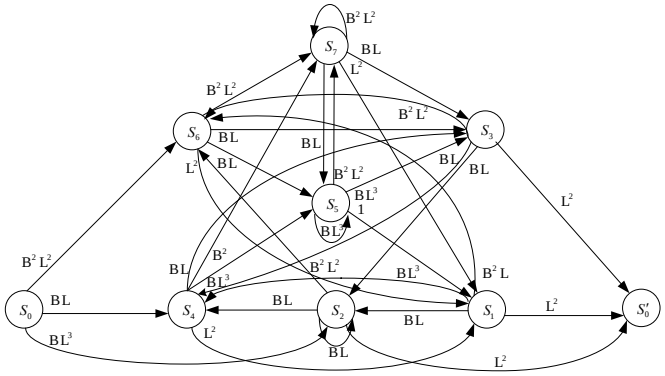

Figure 8: The augment state diagram for CC(1,15/17) with R_c=0.67.

(iii) Upon solving these equations for the ratio S_0'/S_0, we obtain the transfer function for convolutional code with a certain code rate. From this transfer function, we determine a weight enumerator of the CC(1,15/17) with code rate R_c=0.67 as

$$\mathrm{W}_{\mathrm{p}_{0.67}}(B,L) = 2B^2L^3 + BL^4 + 3BL^5 + 2B^2L^5 + 2B^3L^5 + 3BL^6 + B^2L^6 + 5B^3L^6 + ... + B^4L^6 + 2B^2L^7 + 2B^4L^7 + B^5L^7 + B^3L^8 + B^4L^8 + B^2L^9 + B^4L^9$$

The same procedure applies to convolutional codes with a code rate of R_c = 0.2, 0.6, 0.7, 0.9 from mother convolutional code CC(1,15/17) that have puncturing pattern and puncturing period, we also determine the weight enumerator of these codes as

$$\mathrm{W}_{p_{0.2}} = BL^{15} + B^2L^{18} + L^3B^{19} + 2B^2L^{20} + B^3L^{21} + 2B^4L^{22} + 2B^3L^{23} + 2B^4L^{24} + ...$$

$$W_{p_{0.6}}(B,L) = L^5\left(B - B^2 + B^4 - B^7\right) + L^4\left(B^4 - B^3 + B^2\right) - L^3\left(B^2 + B\right) + \ldots$$

$$W_{p_{0.7}}(B,L) = L^5\left(3B^6 + 2B^5 + 2B^4 + 3B^3 + B^2\right) + L^4\left(B^4 + B^2 + B\right) + L^3\left(-B^8 - 7B^7 - 3B^5 - 6B^4 - 6B^3 - 2B^2\right) + L^2\left(-B^7 - B^5 - 2B^3\right) + \ldots$$

$$W_{p_{0.9}}(B,L) = L^5\begin{pmatrix} 4B^{39} + B^{38} + 4B^{37} + 2B^{36} + 17B^{35} + 16B^{34} + 20B^{33} + \\ +20B^{32} + 26B^{31} + 61B^{30} + 40B^{29} + 65B^{28} + 35B^{27} + \\ +101B^{26} + 85B^{25} + 111B^{23} + 77B^{22} + \ldots + 10B^5 + 6B^4 \end{pmatrix} + L^4\left(3B^{20} + B^{29} + 3B^{28} + 2B^{27} + 8B^{26} + \ldots + 5B^3 + 6B^2 + 1\right) + L^3\left(B^{17} + B^{16} + B^{15} + B^{14} + B^4\right) + L^2\left(B^{12} + B^{10} + B^8 + B^6 + B^2\right) + \ldots$$

Weight Enumerator for URC using QPSK modulation

Fig. 9a shows the state diagram for URC with constraint length K=2 and the generator polynomials G=[2/3]. In this case we consider two dummy variables D_1 and D_2. The resulting branch metrics for each branch of URC are shown in Fig. 10c, where the exponent of B represents the Hamming distance of the input sequence.

As shown in Fig.9c, for QPSK modulation scheme (M=4), the merged inner trellis has two states and M/2 parallel edges between every distinct starting and ending state. Accordingly, the weight enumerating function of the inner code (URC) can be given by

$$W(L,D_1,D_2) = \sum_{l}\sum_{m_1}\sum_{m_2} b_{l,m_1,m_2} L^l D_1^{m_1} D_2^{2m_2} \qquad (7)$$

where b_{l,m_1,m_2} is the number of error events consists of m_1 symbols of m_1 Hamming distance and m_2 symbols of $2m_2$ Hamming distance when the input Hamming distance is i.

Then, the weight enumerating function of the inner code URC(2/3) will be

$$\begin{aligned} W(L,D_1,D_2) &= \frac{2LD_1(LD_1 + LD_2)}{1 - L^2D_1 - D_2} \\ &= 2L^2D_1\left(D_2^5 + D_2^4 + D_2^3 + D_2^2 + D_2\right) + \\ &+ 2L^2D_1^2\left(D_2^5 + D_2^4 + D_2^3 + D_2^2 + D_2 + 1\right) + \\ &+ 2L^4D_1^2\left(5D_2^5 + 4D_2^4 + 3D_2^3 + 2D_2^2 + D_2\right) + \\ &+ 2L^4D_1^3\left(6D_2^5 + 5D_2^4 + 4D_2^3 + 3D_2^2 + 2D_2 + 1\right) + \\ &+ 2L^6D_1^4\left(21D_2^5 + 15D_2^4 + 10D_2^3 + 6D_2^2 + 3D_2 + 1\right) + \\ &+ 2L^6D_1^3\left(15D_2^5 + 10D_2^4 + 6D_2^3 + 3D_2^2 + D_2\right) + \\ &+ 2L^8D_1^5\left(56D_2^5 + 35D_2^4 + 20D_2^3 + 10D_2^2 + 4D_2 + 1\right) + \\ &+ 2L^8D_1^4\left(35D_2^5 + 20D_2^4 + 10D_2^3 + 4D_2^2 + D_2\right) + \ldots \\ &+ 2L^{18}D_1^{10}(1287D_2^5 + 495D_2^4 + 165D_2^3 + 45D_2^2 + 9D_2 + 1) + \\ &+ 2L^{18}D_1^9\left(495D_2^5 + 165D_2^4 + 45D_2^3 + 9D_2^2 + D_2\right) + \\ &+ 2L^{20}D_1^{11}(2002D_2^5 + 715D_2^4 + 220D_2^3 + 55D_2^2 + 10D_2 + 1) + \\ &+ 2L^{20}D_1^{10}\left(715D_2^5 + 220D_2^4 + 55D_2^3 + 10D_2^2 + D_2\right) + \\ &+ 2L^{22}D_1^{12}(3003D_2^5 + 1001D_2^4 + 286D_2^3 + 66D_2^2 + 11D_2 + 1) + \\ &+ 2L^{22}D_1^{11}\left(1001D_2^5 + 286D_2^4 + 66D_2^3 + 11D_2^2 + D_2\right) + \\ &+ 2L^{24}D_1^{13}(4368D_2^5 + 1365D_2^4 + 364D_2^3 + 78D_2^2 + 12D_2 + 1) + \\ &+ 2L^{24}D_1^{12}\left(1365D_2^5 + 364D_2^4 + 78D_2^3 + 12D_2^2 + D_2\right) + \\ &+ 2L^{26}D_1^{14}(6188D_2^5 + 1820D_2^4 + 455D_2^3 + 91D_2^2 + 13D_2 + 1) + \\ &+ 2L^{26}D_1^{13}\left(1820D_2^5 + 455D_2^4 + 91D_2^3 + 13D_2^2 + D_2\right) + \\ &+ 2L^{28}D_1^{15}(8568D_2^5 + 2380D_2^4 + 560D_2^3 + 103D_2^2 + 14D_2 + 1) + \\ &+ 2L^{28}D_1^{14}\left(2380D_2^5 + 560D_2^4 + 103D_2^3 + 14D_2^2 + D_2\right) + \ldots \end{aligned}$$

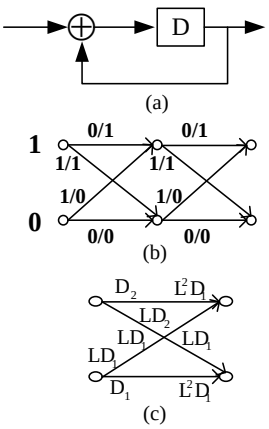

Figure 9: Trellis merging for the inner code.

The weight enumerator for a SCCC with code rates R_c=0.67, 0.2, 0.6, 0.7 and 0.9 employing QPSK modulation is

$$W_{0.67}(B,D_1,D_2)=\frac{2}{\binom{N}{4}}BD_1^2\left(5D_2^5+4D_2^4+3D_2^3+2D_2^2+D_2\right)+$$
$$+\frac{2}{\binom{N}{4}}BD_1^3\left(6D_2^5+5D_2^4+4D_2^3+3D_2^2+2D_2+1\right)+$$
$$+\frac{2}{\binom{N}{6}}D_1^4\left(3B+B^2+5B^3+B^4\right)\left(21D_2^5+15D_2^4+10D_2^3+6D_2^2+3D_2+1\right)+$$
$$+\frac{2}{\binom{N}{6}}D_1^3\left(3B+B^2+5B^3+B^4\right)\left(15D_2^5+10D_2^4+6D_2^3+3D_2^2+D_2\right)+$$
$$+\frac{2}{\binom{N}{8}}D_1^5\left(B^3+B^4\right)\left(56D_2^5+35D_2^4+20D_2^3+10D_2^2+4D_2+1\right)+$$
$$+\frac{2}{\binom{N}{8}}D_1^4\left(B^3+B^4\right)\left(35D_2^5+20D_2^4+10D_2^3+4D_2^2+D_2\right)+\ldots$$

$$W_{0.2}(B,D_1,D_2)=\frac{2}{\binom{N}{18}}B^2D_1^{10}(1287D_2^5+495D_2^4+165D_2^3+45D_2^2+9D_2+1)+$$
$$+\frac{2}{\binom{N}{18}}B^2D_1^9\left(495D_2^5+165D_2^4+45D_2^3+9D_2^2+D_2\right)+$$
$$+\frac{4}{\binom{N}{20}}B^2D_1^{11}(2002D_2^5+715D_2^4+220D_2^3+55D_2^2+10D_2+1)+$$
$$+\frac{4}{\binom{N}{20}}B^2D_1^{10}\left(715D_2^5+220D_2^4+55D_2^3+10D_2^2+D_2\right)+$$
$$+\frac{4}{\binom{N}{22}}B^4D_1^{12}(3003D_2^5+1001D_2^4+286D_2^3+66D_2^2+11D_2+1)+$$
$$+\frac{4}{\binom{N}{22}}B^4D_1^{11}\left(1001D_2^5+286D_2^4+66D_2^3+11D_2^2+D_2\right)+$$
$$+\frac{4}{\binom{N}{24}}B^4D_1^{13}(4368D_2^5+1365D_2^4+364D_2^3+78D_2^2+12D_2+1)+$$
$$+\frac{4}{\binom{N}{24}}B^4D_1^{12}\left(1365D_2^5+364D_2^4+78D_2^3+12D_2^2+D_2\right)+$$

$$W_{0.6}(B,D_1,D_2)=\frac{2}{\binom{N}{4}}D_1^2\left(B^4-B^3+B^2\right)\left(5D_2^5+4D_2^4+3D_2^3+2D_2^2+D_2\right)+$$
$$+\frac{2}{\binom{N}{4}}D_1^3\left(B^4-B^3+B^2\right)\left(6D_2^5+5D_2^4+4D_2^3+3D_2^2+2D_2+1\right)$$

$$W_{0.7}(B,D_1,D_2)=\frac{2}{\binom{N}{2}}D_1\left(D_2^5+D_2^4+D_2^3+D_2^2+D_2\right)\left(-B^7-B^5-2B^3\right)+$$
$$+\frac{2}{\binom{N}{2}}D_1^2\left(D_2^5+D_2^4+D_2^3+D_2^2+D_2+1\right)\left(-B^7-B^5-2B^3\right)+$$
$$+\frac{2}{\binom{N}{4}}D_1^2\left(5D_2^5+4D_2^4+3D_2^3+2D_2^2+D_2\right)\left(B^4+B^2+B\right)+$$
$$+\frac{2}{\binom{N}{4}}D_1^3\left(6D_2^5+5D_2^4+4D_2^3+3D_2^2+2D_2+1\right)\left(B^4+B^2+B\right)$$

$$W_{0.9}(B,D_1,D_2)=\frac{2}{\binom{N}{4}}D_1^3\left(6D_2^5+5D_2^4+4D_2^3+3D_2^2+2D_2+1\right)\left(\begin{matrix}3B^{20}+B^{29}+3B^{28}+2B^{27}\\+8B^{26}+\ldots+5B^3+6B^2+1\end{matrix}\right)+$$
$$+\frac{2}{\binom{N}{4}}D_1^2\left(5D_2^5+4D_2^4+3D_2^3+2D_2^2+D_2\right)\left(\begin{matrix}3B^{20}+B^{29}+3B^{28}+2B^{27}+\\8B^{26}+\ldots+5B^3+6B^2+1\end{matrix}\right)+$$
$$+\frac{2}{\binom{N}{2}}D_1^2\left(D_2^5+D_2^4+D_2^3+D_2^2+D_2+1\right)(B^{12}+B^{10}+B^8+B^6+B^2)+$$
$$+\frac{2}{\binom{N}{2}}D_1\left(D_2^5+D_2^4+D_2^3+D_2^2+D_2\right)(B^{12}+B^{10}+B^8+B^6+B^2)+$$

Pairwise Error Probability over a two-state switched channel

A two-state switched model discussed in Section 2 with the same parameters as noted in [3] in relation to the transition matrix of the Markov process with stationary probabilities π = (0.565 0.435). The first state with stationary probability 0.565 considers frequency-flat uncorrelated real Rician fading channel with Rice factor K = 10dB, while the second state consider frequency-flat uncorrelated real Rayleigh fading conditions. So Pairwise Error Probability (PEP) using QPSK modulation over this two-state switched channel $P_{m_1m_2,QPSK,Two\text{-}state\,switched}\left(X,X\right)$ can be expressed as

$$P_{m_1m_2,QPSK,Two\text{-}state\,switched}\left(X,X\right)=\sum_{m_2}\sum_{m_1}\left(\begin{matrix}0{,}565.P_{m_1m_2,QPSK,Rician}\left(X,X\right)+\\0{,}435.P_{m_1m_2,QPSK,Ray}\left(X,X\right)\end{matrix}\right) \quad (8)$$

For Rayleigh Fading Channel, PEP is expressed as

$$P_{m_1m_2,QPSK,Ray}\left(X,X\right)=\frac{1}{\pi}\int_0^{\pi/2}\left(\frac{\sin^2\theta}{\sin^2\theta+E_s/2N_0}\right)^{m_1}\left(\frac{\sin^2\theta}{\sin^2\theta+E_s/N_0}\right)^{m_2}d\theta \quad (9)$$

For Rician Fading Channel, the conditional pairwise error probability can be written as

$$P_{m_1m_2,QPSK,Rician}\left(X,X\left|\{a_i\}\right.\right)=Q\left(\sqrt{\frac{\frac{E_s}{2N_0}}{\left[\sum_l^{m_1}a_l^2\left|x_l-x_l\right|^2+\sum_k^{m_2}a_k^2\left|x_k-x_k\right|^2\right]}}\right) \quad (10)$$

For using QPSK modulation, $\left|x_l-x_l\right|^2=2$ for m_1 symbols of S_1 and $\left|x_k-x_k\right|^2=4$ for m_2 symbols of S_2. Substituting these values in (7) and using the exact Q function integral, can be written as

$$P_{m_1m_2,QPSK,Rician}\left(X,X\right)=E\left(P_{m_1m_2,QPSK,Rician}\left(X,X\left|\{a_i\}\right.\right)\right) \quad (11)$$
$$=\frac{1}{\pi}\int_{a_1}\ldots\int_{a_{m_1}}\int_{a_1}\ldots\int_{a_{m_2}}\int_0^{\pi/2}\exp\left(-\frac{E_s/2N_0\sum_{l=1}^{m_1}a_l^2}{\sin^2\theta}\right)\ldots$$
$$\ldots\exp\left(-\frac{E_s/N_0\sum_{k=1}^{m_2}a_k^2}{\sin^2\theta}\right)d\theta p_{a_1}\ldots p_{a_{m_1}}d_{a_1}\ldots d_{a_{m_1}}p_{a_1}\ldots p_{a_{m_2}}d_{a_1}\ldots d_{a_{m_2}}$$

substituting the normalized Rician probability density function, we have

$$P_{m_1m_2,QPSK,Rician}\left(X,X\right)=\frac{1}{\pi}\int_0^{\pi/2}2a\left(1+K\right)e^{-K}\left[\int_0^{\infty}\frac{I_0\left(2a\sqrt{K\left(1+K\right)}\right)}{\exp\left(a^2\left[1+K+\frac{E_s/2N_0}{\sin^2\theta}\right]\right)}da\right]^{m_1}\ldots \quad (12)$$
$$\ldots 2a\left(1+K\right)e^{-K}\left[\int_0^{\infty}\frac{I_0\left(2a\sqrt{K\left(1+K\right)}\right)}{\exp\left(a^2\left[1+K+\frac{E_s/N_0}{\sin^2\theta}\right]\right)}da\right]^{m_2}d\theta$$

which after integration reduces to

$$P_{m_1m_2,QPSK,Rician}\left(X,X\right)=\frac{1}{\pi}\int_0^{\pi/2}\left[\frac{\rho_1\sin^2\theta}{1+\rho_1\sin^2\theta}\exp\left(\frac{-K}{1+\rho_1\sin^2\theta}\right)\right]^{m_1} \quad (13)$$
$$\left[\frac{\rho_2\sin^2\theta}{1+\rho_2\sin^2\theta}\exp\left(\frac{-K}{1+\rho_2\sin^2\theta}\right)\right]^{m_2}d\theta$$

where

$$\rho_1=\frac{1+K}{E_s/2N_0}\ ;\ \rho_2=\frac{1+K}{E_s/N_0}$$

So bit error probability of IrCC-URC-QPSK coding scheme in HAP system over two-state switched channel model using 8-subcode IrCC (1,15/17) as

$$P_{e\_\mathrm{IrCC-URC-QPSK}}=\alpha_1P_{e\_0.2}+\alpha_5P_{e\_0.6}+\alpha_6P_{e\_0.7}+\alpha_8P_{e\_0.9} \quad (14)$$

where $P_{e\_0.2}, P_{e\_0.6}, P_{e\_0.7}, P_{e\_0.9}$ is calculated in (5) and weighting coefficients α_i is determined in Fig.4.

Results of performance analysis over the upper bound with simulation results for the HAP system using QPSK modulation over a two-state switched channel model are shown in Fig.10. It is shown that the bit error probability is closer to the simulated BER performance as SNR increases. Furthermore, bit error probability decreases considerably as frame length increases and bit error probability of system IrCC-URC-QPSK significantly improves compared to system CC-URC-QPSK. However, the derived analytic expression is a weak upper bound on the bit error probability. Because the decoding algorithm and type of interleaver are used in simulation and analysis is different.

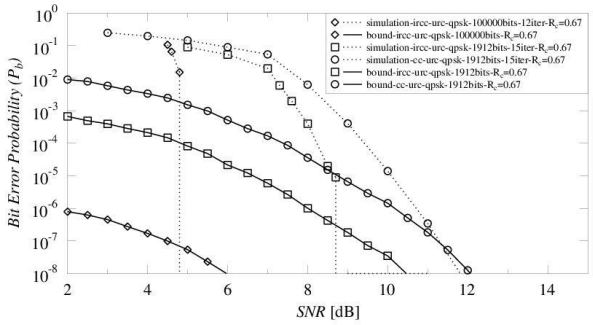

Figure 10: Upper bound on bit error probability for code rate-0.67 CC(1,15/17) and IrCC(1,15/17) codes with QPSK modulation scheme in two-state switched channel model of HAP systems.

CONCLUSIONS

In this paper, we have proposed a modified trellis diagram for punctured convolutional code to determine the transfer function. From this we derived upper bounds for IrCC-URC-QPSK coding scheme for HAP system over two-state switched channel model in terms of maximum-likelihood bit error probability. The obtained results, compared to the simulation results. This comparison demonstrates the accuracy of the presented analysis and vice versa. Although, the derived analytic expression is a weak upper bound on the bit error probability. But, it still shows the effects on the code by frame length, and when using irregular convolutional code. Therefore, this method of analysis is still considered as a tool to design the channel code.

ACKNOWLEDGEMENT

The authors would like to thank to Motorola Solutions Foundation for supporting this research.

REFERENCES

[1]. A. Boch, M. Laddomada, M. Mondin, and F. Daneshgaran, “Advanced channel coding for hap-based broadband services [internetworking and resource management in satellite systems series],” IEEE Aerospace and Electronic Systems Magazine, vol. 22, no. 9, pp. C–7, 2007.

[2]. F. Dong, Y. He, X. Zhou, Q. Yao, and L. Liu, “Optimization and design of HAPs broadband communication networks,” in 2015 5th International Conference on Information Science and Technology (ICIST), pp. 154–159, IEEE, 2015.

[3]. D. Grace and M. Mohorcic, Broadband Communications via High Altitude Platforms. John Wiley & Sons, 2011.

[4]. F. A. Oliveira, F. C. L. d. Melo, and T. C. Devezas, “High altitude platforms present situation and technology trends,” Journal of Aerospace Technology

and Management, vol. 8, no. 3, pp. 249–262, 2016.

[5]. Zheng, Jian Yun, Kai Ji, and Yi Sheng Zhu. "High Altitude Platform-Based Communication System under LDPC Coding in DVB-S2 Standard." Applied Mechanics and Materials. Vol. 602. Trans Tech Publications, 2014.

[6]. M. Tuchler and J. Hagenauer, "Exit charts of irregular codes," 2002

[7]. S. Ten Brink, "Designing iterative decoding schemes with the extrinsic information transfer chart," AEU Int. J. Electron. Commun, vol. 54, no. 6, pp. 389–398, 2000.

[8]. M. El-Hajjar and L. Hanzo, "Exit charts for system design and analysis," IEEE Communications Surveys & Tutorials, vol. 16, no. 1, pp. 127–153, 2014..

[9]. H. V. Nguyen, C. Xu, S. X. Ng, and L. Hanzo, "Near-capacity wireless system design principles," IEEE Communications Surveys & Tutorials, vol. 17, no. 4, pp. 1806–1833, 2015.

[10]. S. Benedetto and G. Montorsi, "Unveiling turbo-codes: Some results on parallel concatenated coding schemes," IEEE Trans. Inform. Theory, vol. 43, pp. 409–428, Mar. 1996.

[11]. D. Divsalar, S. Dolinar, R. J. McEliece, and F. Pollara, "Transfer function bounds on the performance of turbo codes," Jet Propulsion Lab., Pasadena, CA, TDA Progress Report 42-122, pp. 44–55, Aug. 15, 1995.

[12]. J.L. Cuevas-Ruiz and J.A. Delgado-Penin, "Channel model based on semi-Markovian processes. An approach for HAPs systems," In Proc.

of CONIELECOMP, pp. 52-56, 16-18 Feb. 2004.

[13]. Tuchler, Michael, "Design of serially concatenated systems depending on the block length." IEEE Transactions on Communications 52.2 (2004): 209-218.

[14]. S. Benedetto, D. Divsalar, G. Montorsi, F. Pollara, "Serial concatenation of interleaved codes: Performance analysis, design and iterative decoding," IEEE Transactions on Information Theory, Vol. 44, pp. 909-926, May 1998.